Optical Properties of Uncapped InN Nanodots Grown at Various Temperatures

2009 Jpn. J. Appl. Phys. 48 031001

(http://iopscience.iop.org/1347-4065/48/3R/031001)

Optical Properties of Uncapped InN Nanodots Grown at Various Temperatures

Ching-Yu Chen, Ling Lee, Shin-Kai Tai, Shao-Fu Fu, Wen-Cheng Ke, Wu-Ching Chou, Wen-Hao Chang, Ming-Chih Lee, and Wei-Kuo Chen*

Department of Electrophysics, National Chiao Tung University, Hsinchu 300, Taiwan, Republic of China

Received March 1, 2008; accepted September 13, 2008; published online March 23, 2009

Photoluminescence (PL) measurements were employed to investigate the emission properties of uncapped InN nanodot samples grown at temperature from 550 to 725 °C. Our results indicate that once the In droplets are formed, the optical properties of InN dots deteriorate markedly. As for those droplet-free samples grown at temperatures ≥600 °C, good luminescence properties are obtained. The corresponding 20 K PL peak energy is found to be almost constant at approximately 0.77 eV with a slow increase in its linewidth from 71 to 74 meV. A strong temperature-induced energy blue shift at approximately 20 to 280 K is considered to be partially connected to the band-filling effects of thermally stimulated surface electrons. © 2009 The Japan Society of Applied Physics

DOI: 10.1143/JJAP.48.031001

1. Introduction

Recently, indium nitride has received considerable attention because of its superior intrinsic properties, such as narrow direct band gap, low effective mass, high electron mobility, and large drift velocity.[1,2] In addition, the use of InN and its alloys with GaN and AlN can extend its emission from the UV to the near-infrared wavelength, making it very suitable for the fabrication of light-emitting devices covering a wide spectral region. Nevertheless, compared with other nitride semiconductors, an InN binary compound remains one of the least studied materials owing to the low dissociation temperature, high saturation vapor pressure of nitrogen, and high In escaping rate associated with this type of material.[3,4] Even fewer results have been reported on the preparation and physical properties of its nano scale structures. The first emission properties of InN dots were reported in 2005 in a study by Ruffenach *et al.* involving metalorganic vapor phase epitaxy (MOVPE),[5] in which the photoluminescence (PL) peak energy of InN dots encapsulated by SiO_2 was found to be almost invariant to the measured temperature. The size tunable emission properties of InN dots, indicative of quantum size effect, have recently been realized by Ke *et al.* in 2006.[6] The associated peak energy was observed to blueshift systematically from 0.78 to 1.07 eV as the average dot height was tuned from 32.4 to 6.5 nm. On the other hand, the optical behaviors of InN nanodots directly exposed to air, i.e., without any capping layer, have not yet been reported. The uncapped surface quantum dots usually exihibit much weaker and broader PL properties than the capped ones, owing to the existence of a high density of traps on the surface. In this work, we thus devote ourselves to the study of uncapped InN nanodots by focusing on the dependence of their optical properties on growth temperature. Temperature-dependent PL measurement reveals that InN nanodots with good optical properties can be achieved in a wide growth temperature range, even at temperatures as high as 725 °C.

2. Experimental Methods

The uncapped InN dot samples were grown on 1-μm-thick GaN buffer layer/sapphire (0001) substrates by flow-rate modulated epitaxy (FME) with six growth cycles at temperatures varying from 550 to 725 °C. The gas flow sequence for one growth cycle consists of four steps: 20 s trimethylindium (TMIn) step, 20 s NH_3 step, intervened with a 10 s nitrogen carrier gas purge in between. The TMIn and NH_3 flow rates were 150 and 18000 sccm for the In and N steps, respectively. During the TMIn step, a small amount of NH_3 at a flow rate of 500 sccm was also provided to suppress the re-evaporation of In atoms in this step. The TMIn step is also referred to as the growth step because of the deterministic nature of group-III elements in III–V compound growth, whereas the NH_3 step is referred to as the annealing step, in which abundant NH_3 is supplied to convert the unreacted In atoms from the previous growth step into an InN form. The PL measurements were performed using the 488 nm line of an argon-ion laser as an excitation source. The PL signals analyzed by a 0.5 m monochromator were detected by an InGaAs photodiode with a cutoff wavelength of 2.05 μm. The surface structures were examined by an NT-MDT atomic force microscopy (AFM) system, and images were taken using the noncontact tapping mode with a silicon cantilever.

3. Results and Discussion

There is no doubt that growth temperature is a key parameters in determining the epitaxial properties of grown films and their nanostructures. We thus grew InN dots by FME at temperatures from 550 to 725 °C. The resulting AFM micrographs are shown in Fig. 1. As can be seen in the figure, truncated hexagonal InN nanodots, faceted by $\{10\bar{1}2\}$ or $\{10\bar{1}3\}$ planes, spread on the surfaces of all the samples. In droplets, formed either directly on the GaN surface or piled on the top surfaces of InN islands, occur only in samples grown at temperatures ≤575 °C. The corresponding structural properties, determined from AFM micrographs, and electron concentrations, estimated by analyzing the 20 K PL spectra using a line-shaped model,[7] are summarized in Table I. The average height for these dots ranges from 19 to 38 nm and their average diameter is between 180 and 263 nm. Much larger heights were attained for metallic In droplets. Their heights and diameters are 138/311 and 107/386 nm/nm for samples grown at 550 and 575 °C, respectively. The variation in electron concentration seemingly coincides well with the aforementioned growth regions. Electron concentrations as high as $(4.0-4.2)\times10^{18}\,cm^{-3}$ are observed for those droplet-containing samples prepared at low temperature. The electron concentration decreases to $(2.2-2.3)\times10^{18}\,cm^{-3}$ in the mid-temperature growth region and further decreases to $\sim1.7\times10^{18}\,cm^{-3}$ when

*E-mail address: wkchen@mail.nctu.edu.tw

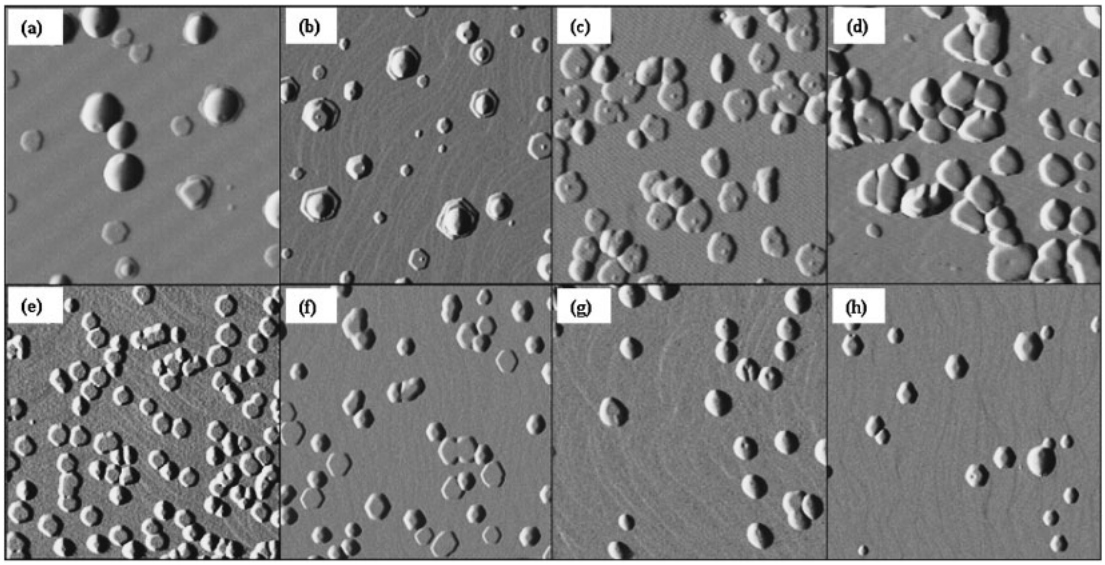

Fig. 1. AFM images of InN dots grown at (a) 550, (b) 575, (c) 600, (d) 625, (e) 650, (f) 675, (g) 700, and (h) 725 °C.

Table I. Average height, diameter, and electron concentration of the InN dots grown at temperatures from 550 to 725 °C. The number in brackets represents the standard deviation of the size distribution in this measurement.

	T_g (°C)							
	550	575	600	625	650	675	700	725
Electron concentration								
n_{op} (10^{18} cm^{-3})	4.0	4.2	2.2	2.3	2.3	2.2	1.9	1.7
InN dots								
H (nm)	25(11)	19(9)	30(14)	26(12)	31(11)	32(12)	33(11)	38(11)
D (nm)	211(50)	180(52)	263(60)	200(65)	233(61)	208(61)	205(56)	196(52)
In droplets								
H (nm)	138(56)	107(48)						
D (nm)	311(82)	386(126)						

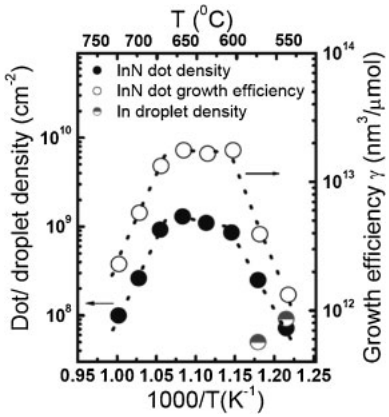

Fig. 2. Arrhenius plots of InN dot density (solid circles) and growth efficiency (open circles) as a function of growth temperature. The In droplet density (gray cirles) is also shown in the figure.

samples were prepared at 725 °C. Figure 2 shows the Arrhenius plot of InN dot density (solid circles) as a function of reciprocal temperature. For comparison, the In growth efficiency (open circles), defined as the ratio of growth rate to input In molar flow rate, is also included in the figure. Three distinct regimes can be clearly observed, namely, low-, mid-, and high-temperature grown regimes, separated by dividing temperatures of ~600 and 650 °C. It can be seen that the dot density increases markedly from 7×10^7 to 8×10^8 cm^{-2} as the growth temperature increases from 550 to 600 °C. It tends to increase slightly in the temperature range of 600–650 °C, starts to decrease rapidly at ~675 °C, and eventually disappears of temperatures >730 °C. The sharp decrease in dot density at high temperatures is considered to relate to the thermal etching or fast evaporation of adsorbed In atoms on the surface, as manifested by the observation of the onset of declining growth efficiency at these temperatures, also shown in Fig. 2.

At the low-temperature growth regime, the samples are covered with a high density $(5–9) \times 10^7$ cm^{-2} of cone-shaped In droplets (denoted by half-filled grey circles in Fig. 2), which is further confirmed by double-crystal X-ray measurements, as shown in Fig. 3, where signals of metallic indium (101) and (110) diffraction peaks (34.5 and 31.3°) are clearly observed, in addition to those observed in the X-ray spectra of sapphire (006), 41.6°, GaN (001), 34.5°, and InN (002), 31.3°. The formation of droplets at low growth temperatures indicates an insufficient supply of active nitrogen radicals during deposition, stemming from

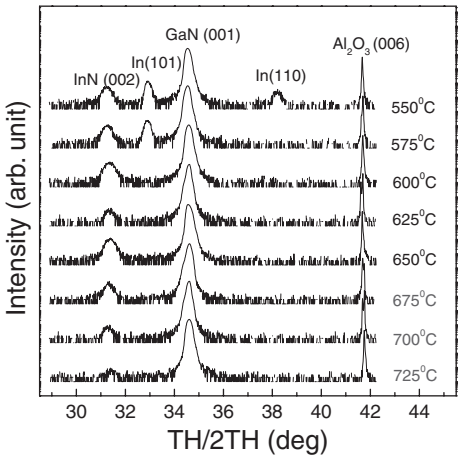

Fig. 3. Double-crystal XRD data ($\theta/2\theta$ scan) of InN dots grown at various temperatures.

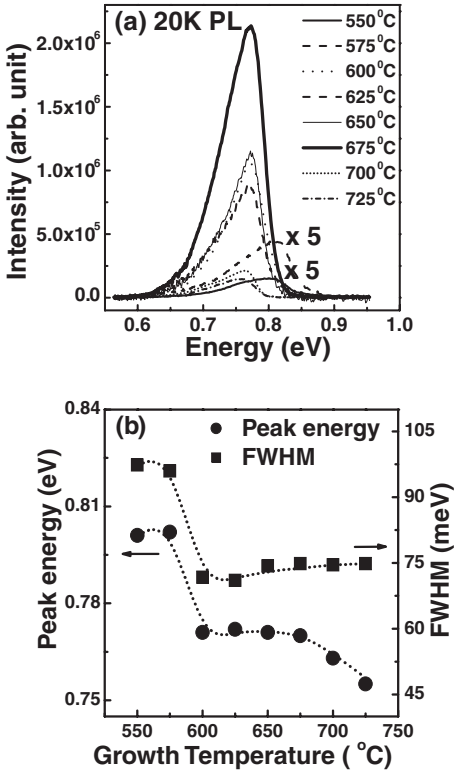

Fig. 4. (a) 20-K PL spectra of InN nanodot samples grown by FME from 550 to 725 °C. The corresponding variations of peak energy and FWHM against growth temperature are shown in (b).

the poor cracking efficiency of NH_3 for temperatures $<575\,^{\circ}C$. Regarding the high-temperature growth regime ($>650\,^{\circ}C$), one may expect the reappearance of In droplets on the surface as observed in conventional InN MOCVD growth, which has been proposed to be due to by the highly unstable nature of the InN material itself at these temperatures.[8] However, this is not observed in our FME-grown InN samples. Neither In droplets nor their X-ray signals were observed. Our results suggest that the use of an FME scheme in InN dot growth, particularly the NH_3 step, can suppress to a certain extent the decomposition of InN at high growth temperatures and concurrently provide a way for unreacted In adatoms to change into the InN form.

The 20 K PL spectra for the above-described InN nanodots are shown in Fig. 4(a). The peak energies and full widths at half maximum (FWHMs) are shown in Fig. 4(b). Inferior optical properties were obtained for low-temperature-grown samples (550 and 575 °C), whose peak energies are located at approximately 0.80 eV with FWHMs as high as ~100 meV. These emission energies are considerably higher than the reported band gap energy of 0.69 eV,[8] indicative of a strong Burstein–Moss effect due to the high electron concentration in these samples. Such a high electron concentration in these low-temperature-grown samples presumably originates from structural defects, such as stacking faults, voids, pits, or point defects, induced by the formation of In droplets on the surface, similar to the cases of GaAs and GaN systems.[9,10]

When the growth temperature is increased to 600 °C, these dots show marked improvement in their optical properties. Not only the peak energy and FWHM are improved to 0.77 eV and 71 meV, respectively, but also the PL intensity is markedly increased, by almost a tenfold increase in magnitude. The good optical qualities in terms of peak energy and FWHM maintains about the same at temperature from 600 to 650 °C and, exceeding our predictions, extend into the high-temperature growth region (where fast In desorption begins to occur during deposition) with only a slight decrease in peak energy and the slow broadening of PL linewidth. Note that even for InN nanodots grown at 725 °C, the upper limit of our growth temperature, reasonably good optical properties can still be obtained. The 725 °C-grown nanodots PL peak energy and FWHM of 0.75 eV and 74 meV, respectively, are comparable to typical results, 0.70–0.83 eV and 100–150 meV, for InN bulk films prepared by conventional MOVPE, which is generally performed at lower growth temperatures of 540–650 °C.[11–13] The preliminary results for these uncapped InN nanodots are encouraging. Although the linewidths (71–74 meV) are still large, they can already compete with those of the uncapped InAs and InGaAs surface quantum dots (54–150 meV).[14–16] Since the luminescent properties can be markedly improved when dots are well capped by a suitable material, this sheds light onto future device applications of InN nanodots.

To gain more insight into the emission properties of these InN dot samples, we subsequently conducted temperature-dependent PL measurements. The results are plotted in Fig. 5 and compared with those for a 500-nm-thick InN bulk film grown at 625 °C. For the bulk film, the measured peak energy fits well with the Varshini-type band-gap shrinkage feature, $E(T) = E_0 - \alpha T^2/(\beta + T)$ with $\alpha = 5.71 \times 10^{-4}$ eV/K, $\beta = 900$ K, and a PL redshift of ~40 meV. With regard to InN nanodots, small blue shifts or slight shifts are observed for those low- and mid-temperature-grown samples. In contrast, clear redshifts of 15–20 meV are observed for samples grown at high temperatures. The corresponding Varshini's parameters are in the ranges of $(1.3–2.2) \times 10^{-4}$ eV/K and 400–500 K for α and β, respectively.

It has been calculated that the band-gap shrinkage for InN from 0 °C to room temperature due to the effects of lattice dilation and electron-phonon interaction is ~60 meV.[17] Thus, the large deviations of temperature-induced PL shifts

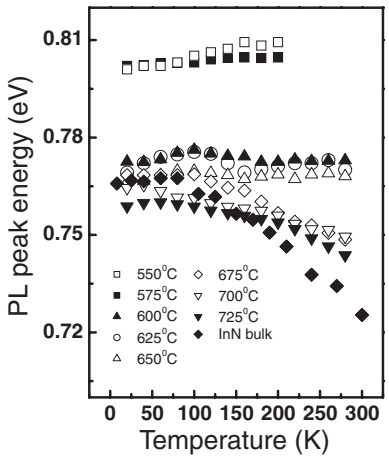

Fig. 5. Temperature dependences of the PL peak energies for our InN nanodot and bulk samples.

from this value strongly suggest that there are blue-shift mechanisms to counterbalance the fundamental band-gap shrinkage in these InN nanodots. The corresponding displacements of peak energy in comparison with the band edge E_0 are approximately 63–68, 60–62, and 40–45 meV for our low-, mid-, and high-temperature-grown InN dot samples, respectively. Such anomalous blue shifts were usually interpreted as the successive filling of localized states[18] and/or band tail states[19] as well as the Coulomb screening of the piezoelectric electric field[20] by photogenerated or thermally released carriers.

The causes of the temperature-induced blue-shift mechanisms of InN nanodots studied here are still unclear at this stage. Aside from the combined effects of the above-mentioned mechanisms, another likely cause is related to the intrinsic property of surface electron accumulation in nanoscale InN dots, which is described as follows. Owing to the high surface state density ($\sim 2.4 \times 10^{13}\,\mathrm{cm}^{-2}$), the results of Cimalla *et al.*[21] indicate that the free electron concentration for a nanoscaled InN crystal (thickness <300 nm) mainly originates from the surface electrons, rather than the bulk electrons. A recent study by Swartz *et al.*[22] also revealed that the surface electron concentration tends to increase significantly when the temperature is increased from 25 to 250 K, in contrast to the small variation for bulk electrons. Consequently, as the measured temperature is increased, more trapped surface electrons are thermally agitated to the conduction band. This gives rise to an alleviated Fermi energy and hence a blue-shifted PL energy for the emitted photons at a higher measured temperature.

Regarding the reduced blue-shift effect observed in the high-temperature samples, we believe that it arise from the fast evaporation of adsorbed In atoms during InN deposition in this temperature range, which produces large densities of In vacancies, acting as acceptors[23] to compensate the thermally stimulated surface electrons in this type of sample.

4. Conclusions

We have investigated the PL properties of uncapped InN nanodots, prepared by flow-rate modulation epitaxy at temperatures from 550 to 725 °C. Our results indicate that the presence of In droplets on the surfaces of the low-temperature-grown samples indeed causes the deterioration the optical properties. As for the high-temperature-grown samples (600–725 °C), where no droplets are formed, reasonably good luminescence results are attained. The corresponding PL peak energy shifts slowly from 0.77 to 0.75 eV with linewidth varying gradually from 71 to 74 meV as the growth temperature increases. Moreover, unlike the small blue shift or absence of variation in the samples grown at temperature <650 °C, clear redshifts of 15–20 meV from 20 to 280 K were observed in our high-temperature InN dot samples, which are rarely seen in nanoscale InN structures.

Acknowledgments

This work is supported in part by the project of MOE-ATU and the National Science Council of Taiwan under grant Nos. NSC 95-2112-M-009-047, NSC 95-2112-M-009-012, NSC 95-2112-M-009-044-MY3, and NSC 95-2112-M-009-020.

1) B. E. Foutz, S. K. O'Leary, M. S. Shur, and L. F. Eadtman: J. Appl. Phys. **85** (1999) 7727.
2) A. G. Bhuiyan, A. Hashimoto, and A. Yamamoto: J. Appl. Phys. **94** (2003) 2779.
3) H. Lu, W. J. Schaff, J. Hwang, H. Wu, W. Yeo, A. M. Pharkya, and L. F. Eastman: Appl. Phys. Lett. **77** (2000) 2548.
4) M. C. Lee, H. C. Lin, Y. C. Pan, C. K. Shu, J. Ou, W. H. Chen, and W. K. Chen: Appl. Phys. Lett. **73** (1998) 2606.
5) S. Ruffenach, B. Maleyre, O. Briot, and B. Gil: Phys. Status Solidi C **2** (2005) 826.
6) W. C. Ke, C. P. Fu, C. Y. Chen, L. Lee, C. S. Ku, W. C. Chou, W. H. Chang, M. C. Lee, W. K. Chen, W. J. Lin, and Y. C. Cheng: Appl. Phys. Lett. **88** (2006) 191913.
7) B. Arnaudov, T. Paskova, P. P. Paskov, B. Magnusson, E. Valcheva, B. Monemar, H. Lu, W. J. Schaff, H. Amano, and I. Akasaki: Phys. Rev. B **69** (2004) 115216.
8) A. G. Bhuiyan, A. Hashimoto, and A. Yamamoto: J. Appl. Phys. **94** (2003) 2779.
9) I. Pietzonka, T. Sass, W. Seifert, S. Gray, and C. Mogensen: Jpn. J. Appl. Phys. **40** (2001) 6531.
10) C. Kruse, S. Einfeldt, T. Bottcher, D. Hommel, D. Rudloff, and J. Christen: Appl. Phys. Lett. **78** (2001) 3827.
11) M. C. Johnson, S. L. Konsek, A. Zettl, and E. D. Bourret-Courchesne: J. Cryst. Growth **272** (2004) 400.
12) A. Yamamoto, K. Sugitaa, H. Takatsuka, A. Hashimoto, and V. Y. Davydov: J. Cryst. Growth **261** (2004) 275.
13) W. J. Wang, H. Miwa, A. Hashimoto, and A. Yamamoto: Phys. Status Solidi C **3** (2006) 1519.
14) B. L. Liang, Z. M. Wang, Y. I. Mazur, G. J. Salamo, E. A. DeCuir, Jr., and M. O. Manasreh: Appl. Phys. Lett. **89** (2006) 043125.
15) I. A. Karpovich, N. V. Baidus, B. N. Zvonkov, S. V. Morozov, D. O. Filatov, and A. V. Zdoroveishev: Nanotechnology **12** (2001) 425.
16) Z. F. Wei, S. J. Xu, R. F. Duan, Q. Li, J. Wang, Y. P. Zeng, and H. C. Liu: J. Appl. Phys. **98** (2005) 84305.
17) A. A. Klochikhin, V. Y. Davydov, V. V. Emtsev, A. V. Sakharov, V. A. Kapitonov, B. A. Andreev, H. Lu, and W. J. Schaff: Phys. Rev. B **71** (2005) 195207.
18) P. G. Eliseev, P. Perlin, J. Lee, and M. Osinski: Appl. Phys. Lett. **71** (1997) 569.
19) P. Perlin, V. Iota, B. A. Weinstein, P. Wisniewski, T. Suski, P. G. Eliseev, and M. Osinski: Appl. Phys. Lett. **70** (1997) 2993.
20) H. Schömig, S. Halm, A. Forchel, G. Bacher, J. Off, and F. Scholz: Phys. Rev. Lett. **92** (2004) 106802.
21) V. Cimalla, V. Lebedev, F. M. Morales, R. Goldhahn, and O. Ambacher: Appl. Phys. Lett. **89** (2006) 172109.
22) C. H. Swartz, R. P. Tompkins, N. C. Giles, T. H. Myers, H. Lu, W. J. Schaff, and L. F. Eastman: J. Cryst. Growth **269** (2004) 29.
23) C. Stampfl, C. G. Van de Walle, D. Vogel, P. Krüger, and J. Pollmann: Phys. Rev. B **61** (2000) R7846.